# Characterizing the Inputs and Functionality of Stress- and Reward-Encoding Neuronal Ensembles in the Ventral Tegmental Area

Diaz Danko
6298737, d,danko@student.uu.nl
MSc Neuroscience & Cognition, Utrecht University
3 November 2023

*Supervisor:* Ioannis Koutlas
*First examiner:* Frank. J. Meye
*Second examiner:* Roger A. H. Adan

**ABSTRACT**

Excessive amounts of stress can contribute to the development and exacerbation of various psychiatric diseases associated with maladaptive reward-driven reinforcement. The ventral tegmental area (VTA) is a mesolimbic brain region that is involved in the integration and processing of both stressful and rewarding experiences and is therefore believed to play a major role in stress-associated psychopathological manifestations. The VTA connectome comprises many synaptic inputs from numerous other brain regions, and it has been demonstrated that these inputs can differ in terms of the emotional valence that they encode. However, it remains elusive to what extent these inputs are engaged in response to a stressful and rewarding experience. The current study characterizes acute social defeat stress- and opioid-responsive neuronal ensembles within brain regions that project to the VTA. It also determines. First, we first quantified stress- and reward-related activation in VTA-projecting brain regions by using targeted recombination in active populations (TRAP2) and showed that acute social stress leads to increased activation in most brain regions whereas mu-opioid receptor agonist (D-Ala2,N-MePhe4,Gly-ol5 enkephalin (DAMGO) administration does not. By utilizing a retrogradely transported adeno-associated virus in combination with TRAP2 to identify monosynaptic VTA afferents responsive to acute social defeat and DAMGO, we found that the fraction of activated medial prefrontal cortex to VTA inputs is higher in the acute social defeat ensemble than in the DAMGO ensemble. Lastly, we sought to determine the functional role of social stress-responsive VTA neurons ($VTA_{SDS}$) in the expression of stress-driven cognitive effects. To that end, we induced the expression of an inhibitory DREADD in the $VTA_{SDS}$-ensemble and demonstrate that inhibition of these neurons during acute social stress precludes the expression of conditioned place aversion.

**LAY SUMMARY**

Health complications due to stress are a common phenomenon in modern society. When experienced in excessive amounts, stress can contribute to the development of psychological diseases such as eating disorders, depression and drug addiction. Individuals that are diagnosed with these disorders typically display abnormal sensitivity for pleasurable experiences, resulting in uncontrolled (de)motivation for rewarding stimuli often at the expense of their own mental and physical wellbeing. Motivation is a reward-driven form of behaviour that is predominantly orchestrated by a neurotransmitter called ''dopamine''. The ventral tegmental area (VTA) is a brain region that harbours a very large population of dopamine-releasing neurons, and therefore acts as an important regulator of motivated behaviour. Dopaminergic neurons in the VTA also receive many neuronal signals from multiple brain regions that can influence their activity, making the dopaminergic signalling system very complex.

Dopamine is commonly acknowledged as the "reward" neurotransmitter, while in reality, dopamine neurons within the VTA are activated by both rewarding and unpleasant experiences, such as stress. Accordingly, multiple studies performed with experimental animals have shown that stress alters dopamine signalling in the VTA and that this translates into stereotypical behaviours associated with depression, addiction and eating disorders. In the last decades, many advancements have been made within the field of neuroscience on how the VTA differentially responds to stressful and rewarding experiences, and how disbalances in this system can contribute to mental illnesses. However, there are still important questions regarding this topic that remain unanswered. For example, from which regions does the VTA receives signals in response to stressful or rewarding experience? Are the sources of these signals different depending on the experience? And would animals behave different in response to stress when their VTA is partially inactive?

In this study, we addressed these questions by utilizing a novel, genetically modified mice in which we could identify neurons that were activated in a stress- or reward-specific context. To create a stressful or rewarding experience, we subjected the mice to territorial aggression or gave them an opioid injections respectively. When looking at brain regions that harbour neuronal connection with the VTA, we saw more neuronal activation in almost every region after stressful experience, but not after the rewarding experience. Next, by using a viral-based technique to visualize neurons that exclusively provide direct signals to the VTA, we wanted to determine whether this stress-dependent increase in neuronal activity was also directly projected to the VTA. We compared the activation between the same stressful and rewarding event, and found that the VTA only receives increased input from the medial prefrontal cortex in response to stress, whereas for the other regions we saw no differences. Lastly, we assessed whether inhibition of stress-responsive neurons in the VTA would have an effect on stress-driven behavioural changes. We inhibited these neurons by injecting the mice with a pharmacological compound, and demonstrated that this procedure completely prevents the formation of a memory associated with a stressful experience.

In sum, our study shows how stress and reward differentially engage neuronal circuits that project to the VTA, and that stress-responsive neurons in the VTA play a functional role in cognitive adaptations to stress. Ulitmately, our findings contribute to the understanding of how the VTA integrates both rewarding and stressful experiences, thereby facilitating future experiments that address the role of stress in the development of psychiatric diseases.

## INTRODUCTION

Social stress is a common risk factor for the pathogenesis and exacerbation of various psychiatric diseases associated with maladaptive reward processing in vulnerable individuals, such as binge eating disorders, drug addiction and depression (Holly & Miczek, 2016; Sinha & Jastreboff, 2013). Over the past decades, it has been extensively demonstrated that stress influences the neural connectome of the reward system through altered synaptic potentiation, neurochemical signalling and gene expression (Baik, 2020; Holly & Miczek, 2016; Meye & Adan, 2014). Nevertheless, an overarching comprehension of how the neural circuits that encode stress and reward are embedded in the brain, and to what extent the disruption between these systems contributes to the development of these psychopathologies, remains obscure.

The ventral tegmental area (VTA) is a brain region, part of the mesolimbic dopamine system that receives and integrates both rewarding and aversive signals from numerous brain regions to facilitate behavioural reinforcement, making it an interesting hub to study the effects of social stress on reward processing (Morales & Margolis, 2017). Despite being mostly dopaminergic, neurons that reside within the VTA do not constitute a uniform population but rather encompass multiple cell types with distinct roles in motivational control (Morales & Margolis, 2017). Moreover, these neurons are directly innervated by a wide variety of monosynaptic inputs from other brain regions (Faget et al., 2016; Watabe-Uchida et al., 2012), and previous work has shown that these inputs can contrastingly differ in terms of the emotional valence that they encode. For example, optical stimulation of neurons projecting from the laterodorsal tegmentum (LTDg) to the VTA evokes conditioned place preference (CPP) in mice, whereas stimulation of lateral habenula (LHb) to VTA projections leads to conditioned place aversion (CPA) (Lammel et al., 2012). On the other hand, opposing emotional stimuli may also engage partly overlapping neuronal networks, as demonstrated by local field potentials recordings within the VTA revealing that roughly 30% of all detected neurons are activated upon exposure to both unexpected sucrose and tail pinching (Del Arco et al., 2020). Furthermore, photometric calcium recordings showed that dopaminergic VTA neurons similarly exhibited increased $Ca^{2+}$ levels in response to both conditioned sucrose and foot shock (Root et al., 2020). Taken together, the abovementioned findings suggest that aversive and rewarding experiences are encoded by distinct afferents that activate converging neuronal populations within the VTA.

Social defeat stress (SDS) is a commonly used experimental paradigm to emulate the physiological and behavioural effect of social stress in animal models (Smith et al., 2023). In rodents, SDS has been shown to induce aberrations in weight gain (Goto et al., 2014; Johnston et al., 2015), the expression of anxious behaviour (Patki et al., 2013), and the development of depression-like phenotypes (Chaudhury et al., 2012). SDS engages the VTA (Koutlas et al., 2022), and it has been demonstrated that SDS-induced neuroadaptive changes in VTA afferents drive the manifestation of stress-dependent behavioural deviances. For instance, laterodorsal tegmentum (LTDg) to VTA inputs appear to be hyperexcitable after SDS, and chemogenetic silencing of this pathway alleviates stress-induced social deficits in mice (Fernandez et al., 2018). Furthermore, recent evidence infers the imperative role of lateral hypothalamus (LH) to VTA projections in stress-induced palatable food consumption, as strengthening of these inputs mimicked the increased fat intake observed after SDS (Linders et al., 2022). SDS also leads to a rapid increase in expression of μ-opioid receptor (MOR) mRNA in VTA (Nikulina et al., 1999). MORs play an important role in opioid-dependent dopamine activity in the VTA and are therefore critically involved in motivational control of behaviour (Fields & Margolis, 2015). Accordingly, MOR agonist administration in the VTA elicits CPP (Y. Zhang et al., 2009) and increased palatable food intake (Lamonte et al., 2002), and these effects are prevented when MOR functioning is blocked. Notably, knock-down of MORs in the VTA has also been shown to alleviate SDS-driven weight gain deficits and social anxiety (Johnston et al., 2015), indicating that the endogenous opioid system partially dictates behavioural responses to stress. Overall, these findings infer that neuroadaptations in the VTA and its inputs play an important role in the expression of stress-induced behavioural abberations, but it

remains unclear which neuronal ensembles in the VTA are responsibe for these stress-dependent effects.

In the present study, we identify and manipulate neuronal ensembles that account for the processing of stressful (acute SDS) or rewarding (μ-opioid receptor agonist; [D-Ala2,N-MePhe4,Gly-ol5] enkephalin [i.e., DAMGO]) experiences by leveraging a transgenic mouse line in which c-Fos driven Cre-recombinase expression is temporally controlled (Targeted Recombinase in Active Populations; TRAP2) (DeNardo et al., 2019). By injecting TRAP2 mice with a retrogradely transported adeno-associated virus ($AAV_{retro}$) carrying a Cre-dependent mCherry transgene in the VTA, we were able to specifically visualize and quantify stress- or reward-responsive neuronal populations that project to the VTA. Moreover, we gained permanent chemogenetic control over an acute SDS-responsive ensemble in the VTA ($VTA_{SDS}$), and demonstrated that silencing these neurons blocks acute SDS-induced conditioned place aversion (CPA), but not SDS-induced fat hypophagia or anxiety. In sum, our findings show to what extent VTA inputs are differentially activated during stressful or rewarding events, and establish a role of the $VTA_{SDS}$-ensemble in the manifestation of acute stress-induced behavioural phenotypes.

## MATERIALS AND METHODS

### Animals

All experiments were performed with adult (> 8 weeks) male mice (25-38 g). C57Bl6J (Jax #664) heterozygous TRAP2 (Jax #030323), heterozygous mice Ai14 reporter Ai14 tdTomato reporter (Jax #007914) double heterozygous TRAP2xAi14 offspring originated from the Jackson Laboratory, but were house-bred. Proven breeder Swiss CD-1 mice were obtained from Janvier (France) to function as aggressors in the social stress paradigm. All mice (except Swiss-CD1 mice) were group-housed in rooms with regulated temperature (22 ± 2°C) and humidity (60-65%), exposed to a 12h light/dark cycle (lights on at 7am) with access to standard laboratory chow [Special Diet Services [SDS], product code CRM(E)] and water *ad libitum*. The experiments in this study all received approval from the Animal Ethics Committee of Utrecht University, and were carried out in agreement with Dutch law (Wet op de Dierproeven, 2014) and European regulations (Guideline 86/609/EEC).

### Stereotactic Injections

Mice were brought under general anesthesia with ketamine (75 mg/kg i.p.; Narketan, Vetoquinol) and dexmedetomidine (1 mg/kg i.p.; dexdomitor, Vetoquinol). Afterwards, mice were locally anesthetized through topical Lidocaine (0.1 ml; 10% in saline; B. Braun) application under the skin on the skull prior to incision. To prevent dehydration of the eyes during surgery, eye ointment cream (CAF, Ceva Sante Animale B.V., Naaldwijk, Netherlands) was applied beforehand. Mice were fixated in a stereotactic frame (UNO B.V., Zevenaar, Netherlands, Model 68U801 or 68U025) and placed on a heating element (33 °C) throughout surgery. Injections were administered through a 31G metal needle (Coopers Needleworks, Birmingham, United Kingdom) connected to a 10 μl Hamilton syringe (model 801RN) via flexible tubes (PE10, 0.28 mm ID, 0.61 mm OD, Portex, Keene, NH, United States). The Hamilton syringe was automatically controlled by a pump (UNO B.V., Zevenaar, Netherlands, - model 220). Animals were bilaterally injected in the VTA (relative to Bregma: 3.2 mm posterior, 1.6 mm lateral, and 4.9 mm ventral) at an 15° angle with 0.3 μl of AAV per hemisphere at a rate of 0.1 μl/min. $rAAV2_{retro}$-hSyn-DIO-mCherry (4.2 x $10^{12}$ gc/ml; UNC Vector Core) was injected in the VTA of TRAP2 mice to visualize monosynaptic inputs to the VTA. rAAV2-hSyn-DIO-hM4D(Gi)-mCherry (4.2 x $10^{12}$ gc/ml; UNC Vector Core) or rAAV2-hSyn-DIO-mCherry (4.2 x $10^{12}$ gc/ml; UNC Vector Core) was injected in the VTA of TRAP2 mice for c21-dependent inhibition of neurons in the VTA or control respectively. After infusion, needles were left in place for 10 minutes, whereafter they were positioned 50 μm before completely

retracting them 30 s later. Next, the mice were sutured (V926H, 6/0, VICRYL, Ethicon) and received subcutaneous injections with atipamezole(50 mg/kg; Atipam, Dechra), carprofen (5 mg/kg, Carporal) and 1 ml of saline. Mice were kept on a heating element (36 °C) to recover. For 7 days after the surgery, carprofen was provided in drinking water. After surgery, mice were placed in solitary housing for 3 days and received carprofen (0.025 mg/l) through drinking water for 7 days. A minimum of 28 days was reserved for post-operative recovery before subjecting the mice to behavioural manipulations. TRAP2 (*n* = 2) mice with misplace injections were excluded from the final analysis (Fig. S2E).

Social Stress Paradigm

Aggressor Swiss-CD1 male mice were housed individually in a Makrolon cage (type IV, Tecniplast, Buguggiate, Italy). Experimental TRAP2 or TRAP2xAi14 mice were placed in the home cage of the CD1 mice between 8:00 – 10:30. Fighting was permitted for an accumulated 20 s as measured by manual timing, whereafter a transparent air-permeable barrier was placed in the cage to cease further physical contact while still allowing sensory perception for the remaining time of the experiment. For TRAPxAi14 an $AAV_{retro}$-TRAP2 experiments animals remained in the D1 aggressor cage until 4-OHT injection (3 h later). Control animals were placed in a Makrolon cage together with a novel male cage, separated from the beginning by a transparent air-permeable barrier and perfused 90 min later.

Mice were housed solitarily for 7 days before the stressful encounter. Within this period, mice were habituated to intraperitoneal (i.p) injections by receiving saline injections i.p. on days 4 and 5. After fighting for 20 s and being separated by a semi-permeable barrier, TRAP2(xAi14) mice were injected with 4-hydroxtamofixen (4-OHT) i.p. at a dose of 25 mg/kg body weight. 4-OHT (Sigma-Aldrich Chemie N.V., Zwijndrecht, Netherlands, H6278) was dissolved in an aqueous solution according to previous methodology (Ye et al., 2016), ultimately containing 2.5 mg/ml 4-OHT in 5% DMSO, 1% Tween-80 and saline. The 4-OHT injection was given 3 h after the start of the social stress episode. Then the mice were placed back in their home cage (solitary housing). For TRAP2xAi14 and $AAV_{retro}$-TRAP2 experiments, mice were transcardially perfused 7-10 days later.

DAMGO injections

Mice were housed solitarily for 7 days before being injected with DAMGO. Again, mice received saline injection i.p. on day 4 and 5 after the start of their solitary housing to habituate them. Next, mice were injected with DAMGO i.p. at a dose of 1mg/kg body weight in their home cage. Control animals received a saline injection (i.p.) of an equivalent volume of 1mg/kg body weight. 2 h after the DAMGO/saline injection, mice were injected with 4-OHT (25mg/kg). For TRAP2xAi14 and $AAV_{retro}$-TRAP2 experiments, mice were transcardially perfused 7-10 days after the DAMGO/saline injection.

Palatable food choice paradigm

Palatable food choice experiments took place in a clean, enrichment-free cages with two metal food plates attached vertically to both opposing outer ends of the cage wall. One plate was mounted with regular chow (3.61 kcal/g) and the other plate was mounted with fat (Blanc de Boeuf, Vandermoortele, 9.0 kcal/g). Before starting the experiment, animals were habituated to the new fat diet for 1 h per day until a baseline rate of fat intake was reached. Intake was measured by weighing the fat before and after the 1 h session. A steady baseline was acknowledged only when the average weight of fat consumed deviated no more than 0.05 g between subsequent days. On the test day, half of the mice received a c21 injection (2 mg/kg ) i.p. and the other half received a saline injection before 15 min before being exposed to the social stress paradigm (as described before). 15 min after the stress episode mice were placed in the feeding cage for 1 hour, whereafter the fat intake was determined. The next day, animals were again placed in the feeding cage for 1 h to measure post-test fat intake. 7 days later, the experiment was repeated in a counter-balanced manner, i.e. the mice that previously received a c21 injection on the test day were now injected with saline and vice versa.

Open Field Test

Open-field experiments were executed in a custom made open field arena which consisted of a square field (87 by 87 cm) and circular wall (251 cm in circumference, 35 cm high). The field of the arena contained white-lined patterns to delineate the center zone (56 cm in circumference) and the peripheral zone (outer border: 251 cm in circumference, inner border; 207 cm in circumference). Mice received a c21 injection (2 mg/kg ) i.p. 15 minutes before being exposed to the social stress paradigm (as described before), and were place in the OF arena 15 minutes later. The mice were left to roam the arena for 10 minutes before translocating them back to their home cage. During the experiment, mice were recorded by a camera situated above the open field arena. Movement was tracked with Ethovision software (Version 11, Noldus Information Technology, the Netherlands).

Place Preference Test

Conditioned place aversion (CPA) experiments were performed in a custom-made 3-compartment rectangular device (74 x 25 cm, 30 cm high) with an open ceiling, for an unforced-choice behavioural paradigm. The middle, neutral zone-compartment separated the other two conditioning zone-compartments, which were distinguishable in wall pattern and floor texture. One test compartment had a vertical white-and black-striped walls and metal grid flooring in square pattern (squares were 0.2 by 0.2 cm) whereas the other test compartment had a black walls metal grid flooring in square patterns (squares were 0.5 by 0.5 cm). The middle compartment had a white wall colour. On the conditioning days (day 1 – 2), two off-white Plexiglas® barriers (24 x 40 cm) were placed bordering the neutral zone so that each compartment was closed off. On the test day (day 3), the barriers were removed so that the mice could roam freely between the compartments.

Following an unbiased approach, on conditioning day 1 of the experiment mice were either placed in the black or striped compartment in the absence of a CD1 aggressor, where they were left to roam freely for 30 minutes. On conditioning day 2, the mice were placed in the other compartment initially undisturbed for 5 min after which a aggressor was introduced in the compartment, After fighting of an accumulated 20 s occurred, or when 10 min elapsed, the aggressor was removed from the compartment. The mice remained in the compartment up until a total of 30 min elapsed before being translocated back to their home cage. On both conditioning days, all animals received an i.p. c21 injection with a dose of 2 mg/kg 15 min prior to being placed in the test compartment. On day 3, CPA was tested by placing the mice in the neutral zone with the barriers removed and tracking their roaming paths within the compartments for 30 min. Mice were recorded by a camera situated above the CPA device and tracked with Ethovision software (Version 11, Noldus Information Technology, the Netherlands).

Immunohistochemistry

Animals were transcardially perfused with 4% paraformaldehyde (PFA) and brains were post-fixated in 4% PFA at 4°C for 24 h. Next, they were translocated to a 30% sucrose solution in PBS in which they were left for a duration of 48 - 72 h. Coronal sections were of 35 µm were made with a cryostat (CM1950, Leica, Netherlands). Slices were first washed 4 x 10 min in PBS whereafter they were incubated in blocking buffer [5% normal goat serum (NGS), 2.5% bovine serum albumin, 0.2% Triton X-100 in PBS] for 1 h. Next slices were transferred to the primary antibody solution consisting of rabbit-anti-RFP (1:500; Rockland Immunochemicals, 600-401-379, Pottstown, PA, United States) and mouse-anti-TH (1:1000; Sigma-Aldrich Chemie N.V, MABB318, Zwijndrecht, Netherlands) in blocking buffer overnight. The subsequent day slices were washed 4 x 10 min in PBS followed by 2 h secondary antibody solution containing goat anti-rabbit Alexa Fluor 568 (1:500; Abcam, ab175471, Waltham, MA, United states) and goat anti-mouse Alexa Fluor 647 (1:500; Thermo Fisher Scientific, A-21236, Waltham, MA , United States). Finally, slices were mounted on glass slides with 0.2% gelatin in PBS and coverslipped using FluorSave (Millipore, 345798, Amsterdam, Netherlands).

Cell Counting

For cell quantification in all experiments, 4-6 hemisections for each region were acquired using a wide-field epifluorescence microscope (AX10, Zeiss). Fiji software (Schindelin et al., 2012) was used to manually delineate the boundaries of the hemisection based on anatomical landmarks and the Paxinos brain atlas (2nd edition; Academic Press). Next, cells expressing tdTomato or mCherry were automatically counted by an experimenter blinded to the experimental conditions. Automatic counting was performed by using the Analyze Particles plug-in (size in microns$^2$: 50-infinity; circularity: 0.20 - 1.00) in Fiji.

Statistical Analysis

Data analysis was executed in GraphPad Prism 9.3.1 (San Diego, CA, United States). Animals were assigned to experimental conditions at random. To test for differences in tdTomato or mCherry expression in VTA inputs regions between control and stress or DAMGO groups, Two-Way ANOVA test with post-hoc Bonferroni's test for multiple comparisons was used. To test for differences in time spent in each CPA compartment, time spent in the open-field center region, distance moved in the open-field arena and fat intake between mCherry and hM4Di groups, Two-Way ANOVA test with post-hoc Bonferroni's test for multiple comparisons was used. Error bars in graphs represent means + SEM alongside individual data point distributions. *P* values lower than 0.05 were considered as significant.

## RESULTS

### Acute Social Defeat Stress, But Not DAMGO Leads to Higher Neuronal Activation in Several Brain Regions that Project to the VTA

First, we wanted to assess to what extent neuronal populations in different brain regions that project to VTA are activated by acute SDS and DAMGO. To achieve this, we utilized Targeted Recombination in Active Populations (TRAP2) transgenic mice (DeNardo et al., 2019). TRAP2 leverages the c-Fos promotor to drive expression of a modified Cre-recombinase (CreER$^{T2}$) which can only be transported back from the cytosol to the nucleus in the presence of 4-hydroxytamoxifen (4-OHT). This enables a system in which Cre-dependent transgene expression in activated neurons can be temporally controlled by injecting 4-OHT at a specific time point (Fig. 1A).

To label stress or opioid reward-activated ensembles, we exposed double transgenic TRAP2xAi14 tdTomato reporter mice to an acute SDS paradigm or administered a DAMGO i.p. injection. In the acute SDS paradigm, the mice were briefly exposed to an aggressor up until a total 20 s of fighting occurred (within 10 min), whereafter the mice were separated with a transparent, perforated barrier. After being exposed to acute SDS or DAMGO, the mice were injected with 4-OHT to induce targeted Cre-dependent expression of tdTomato in neurons that were activated during the aversive/rewarding experience. Afterwards, we perfused the animals and sliced their brain in order to quantify the tdTomato+ neurons (Fig. 1C). We found that neurons in the LH, mPFC and nucleus accumbens (NAc) are significantly more activated by acute SDS than by DAMGO [$F_{(2,126)}$ =40,85; Fig. 1D, E]. Furthermore, we also observed more neuronal activation in the ventral pallidum (VP), bed nucleus of the stria terminalis (BNST), habenula (Hb) and nucleus accumbens (NAc), although not significant (Fig. 1D, E). The dentate gyrus (DG), caudate putamen (CPu) and claustrum (Cl) displayed no differences in neuronal activation between the two stimuli [$F_{(1, 90)}$ = 34,20; Fig. S1A, E], suggesting that the increased neuronal activation by acute SDS is not a brain-wide effect due to the extreme nature of the stress experience, but rather engages certain regions more than others in terms of activation.

We also compared acute SDS and DAMGO to neutral control stimuli – that is – the novel cage mate group and saline injected group combined, and found that acute SDS induces significantly more activation in the mPFC, NAc, BNST, LH and Hb in comparison to controls (Fig. 1D, E). Again, this effect

was region specific to some extent, since this difference was not observed in the DG, CPu and Cl [$F_{(1, 90)}$ = 33,04; Fig. S1B, E]. Contrastingly, neuronal activation compared between DAMGO and control stimuli was similar in all quantified regions (Fig. 1D, E). Importantly, when acute SDS and DAMGO were compared to their respective controls only, similar differences were found [stress vs. cagemate: $F_{(1, 90)}$ = 34,20; DAMGO vs. saline: $F_{(1, 90)}$ = 0,35; Fig. S1B, C). Furthermore, there were no differences in neuronal activation between novel cage mate and saline control groups [$F_{(1, 90)}$ = 1,55; Fig. S1D]. Altogether, these results demonstrate that acute SDS, but not DAMGO leads to more neuronal activity in several VTA-projecting brain regions, and that this is a brain region-specific effect.

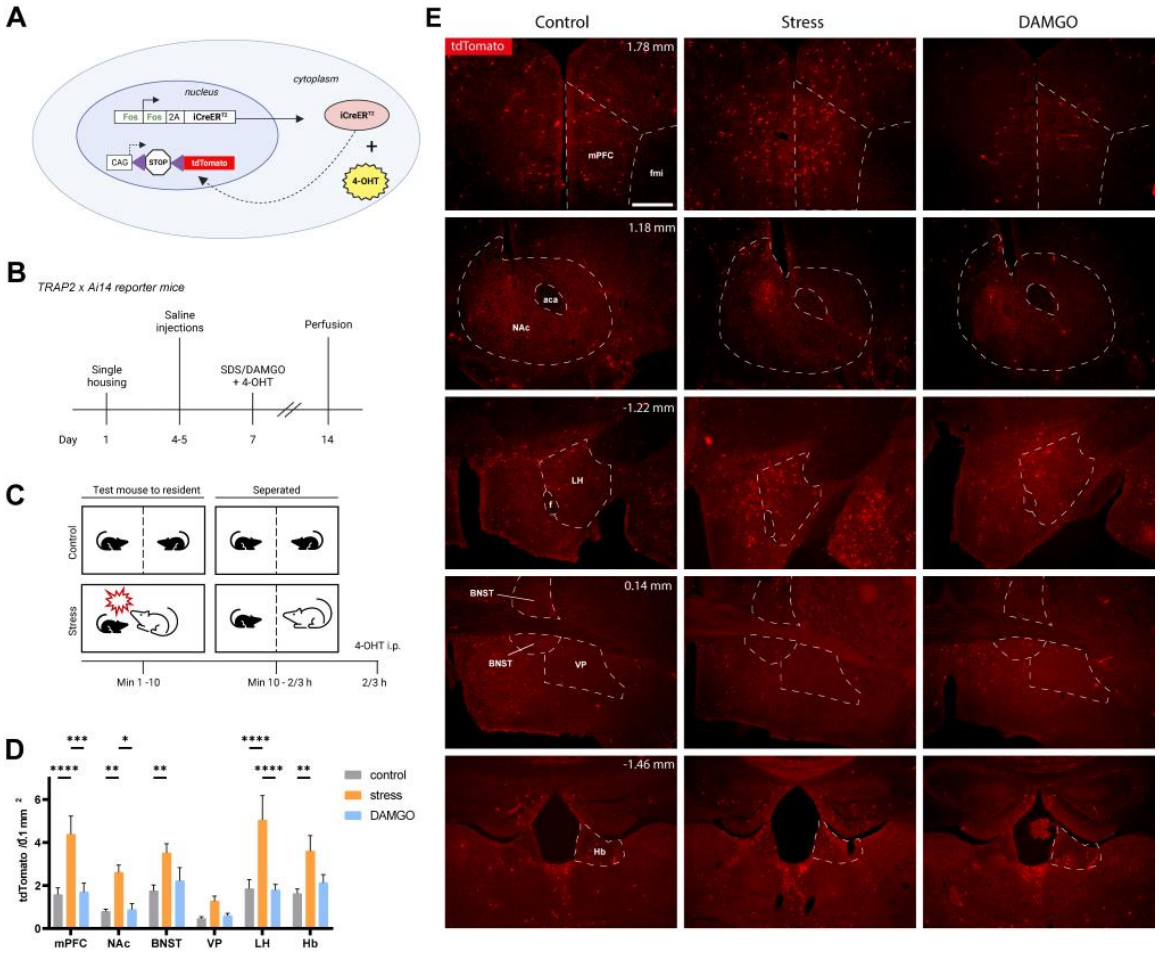


**Figure 1.** Characterization of stress- and DAMGO-activated neuronal ensembles in VTA-projecting brain regions. **(A)** Schematic illustration of TRAP2 mechanism of action. Acute social stress or DAMGO engages a subset of neurons in which iCreER$^{T2}$ becomes (tamoxifen-dependent Cre) expressed due to transcription of the cFos promoter. Upon 4-OHT administration, Cre is transported back into the nucleus where it effectuates recombination of the Lox-P flanked fluorescent tdTomato transgene. **(B)** Experimental timeline of the acute social defeat stress paradigm. **(C)** Experimental timeline of inducing Cre-dependent tdTomato expression in experience-responsive neurons. **(D)** Bar chart quantification of control-, stress- and DAMGO-TRAPed neurons in a selection of VTA-projecting brain regions (neutral: *n* = 12 per group, stress: *n* = 6 per group, DAMGO: *n* = 6 per group). Data are presented as mean +SEM with individual data points (mice) shown alongside of the bars , **P* < 0.05, ***P* < 0.01, ****P* < 0.001, *****P* < 0.0001. Statistics: Two-Way ANOVA and Bonferroni *post-hoc* test. **(E)** Representative images of mPFC, NAc, LH, BNST, VP and Hb sections expressing tdTomato from control-, stress- and DAMGO-exposed TRAP2xAi14 animals. Abbreviations; fmi: corpus callosum, aca: anterior commissure, f: fornix. Scale bar: 500 microns.

**The Acute Social Defeat Stress-Responsive VTA-Input Ensemble Has a Higher Fraction of Activated mPFC Projections than the DAMGO-Responsive Ensemble**

Since several regions that are known to innervate the VTA were significantly more engaged by acute SDS then by DAMGO, we sought to determine whether this effect could be explained by increased activation of neuronal ensembles that project directly to the VTA. To quantify the activation of monosynaptic inputs to the VTA in response to SDS or DAMGO, we injected a retroAAV carrying a loxP-flanked mCherry transgene in the VTA of TRAP2 mice (Fig. 2A). After recovery, we exposed these TRAP2 mice to the acute SDS paradigm or gave them a DAMGO i.p. injection, followed by a 4-OHT i.p. injection to induce c-Fos driven expression of $CreER^{T2}$ in monosynaptic projection to the VTA (Fig. 2A). This allowed for quantification of mCherry-expressing cells, accounting as a direct measure for activated VTA inputs in response to acute SDS or DAMGO.

We found that in terms of total activation, inputs originating from the mPFC were significantly more engaged by acute SDS then by DAMGO [$F_{(1,80)} = 0.024$, $P = 0.012$; Fig. 2C]. This statistical difference was also evident when we analysed fractional activation [$F_{(1,80)} = 0.040$, $P < 0.0001$; Fig. 2D]. However, when accounted for area size, this significance did not hold up [$F_{(1,80)} = 1.696$, $P > 0.999$; Fig. 2B). When compared to the control group (novel cage mate and saline controls combined), no differences with acute SDS or DAMGO were detected in activation relative to the area [$F_{(2,110)} = 1.763$; Fig S2A]. In terms of fractional activation, the DAMGO-activated ensemble encompassed less inputs from the mPFC in comparison to control [$F_{(2,110)} = 0.024$, $P < 0.0001$; Fig S2B]. In terms of total activation, both DAMGO and acute SDS engaged mPFC inputs in a lesser extent than control [$F_{(2,110)} = 3.520$, $P = 0.0112$ (SDS), $P = 0.0118$ (DAMGO); Fig S2C]. However, it should be noted that the control group contained four animals, whereof two were exposed to a novel cage mate, and two received a saline injection. In general, we noted that activated VTA afferents from mid- and hindbrain regions [rostromedial tegmental nucleus (RMTg), dorsal raphe (DR), pedunculopontine tegmental nucleus (PPTg), ventrolateral periaqueductal gray (vlPAG), laterodorsal tegmentum (LDTg)] appeared to be more prevalent in response to acute SDS and DAMGO then the more anterior-located regions (mPFC, BNST, VP, LH, LHb, Fig. 2C). Accordingly, these regions combined constituted the largest fraction of activated VTA inputs in both conditions (Fig. 2E). To our surprise, we saw no mCherry expression the nucleus accumbens (Fig. S2F).

In sum, the quantified VTA inputs in this experiment do not respond differently to acute SDS and DAMGO in terms of quantity relative to the area. In that sense, the increased neuronal activation due to acute SDS as observed in the TRAPxAi14 analysis is not due to increased activation of neuronal populations that specifically project to the VTA. However activated mPFC to VTA inputs are higher both in terms of absolute number and fraction in response to acute SDS versus DAMGO.

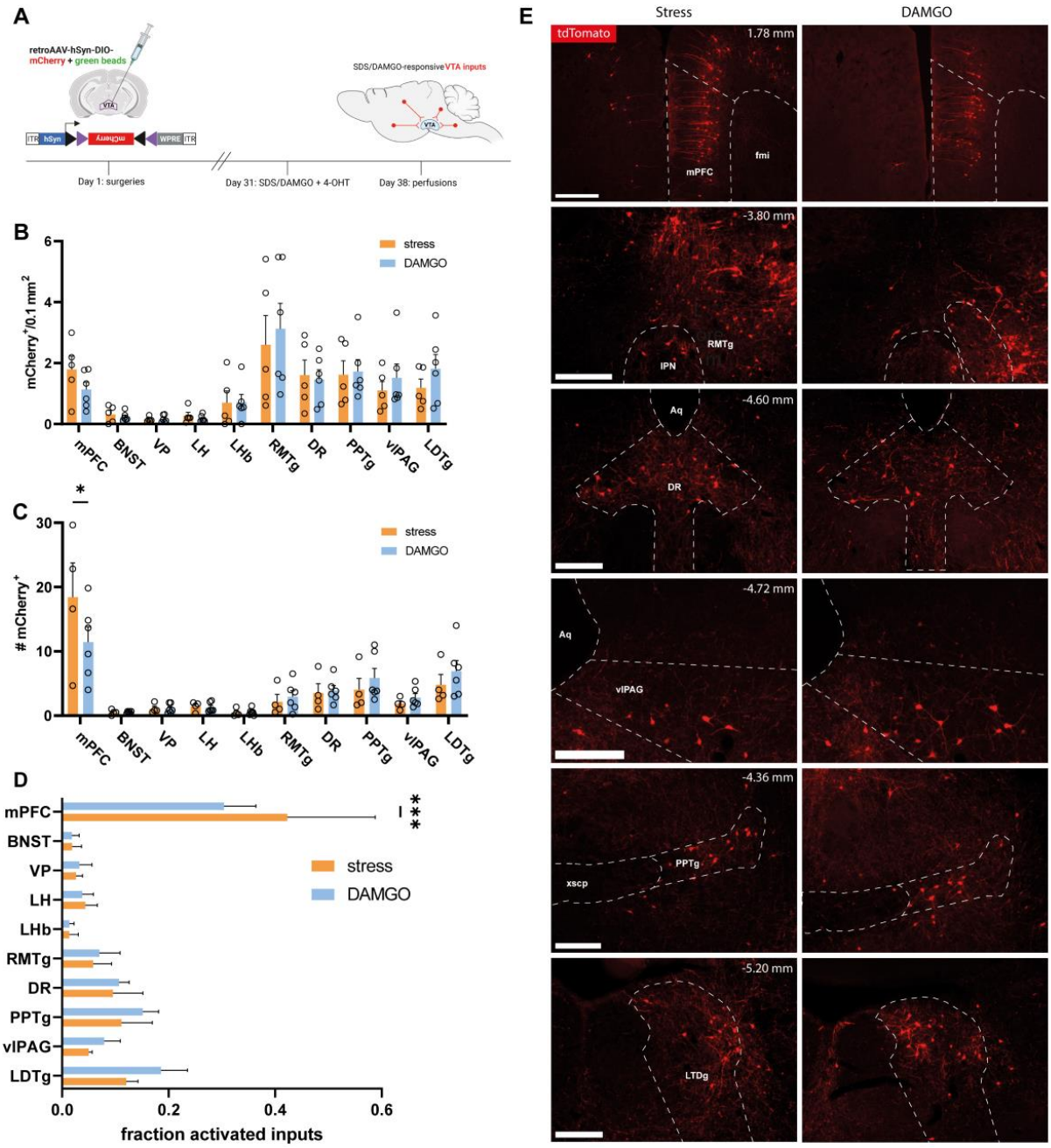


**Figure 2.** Characterization of stress- and DAMGO-activated ensembles of neurons that project directly to the VTA. **(A)** Experimental timeline of inducing Cre-dependent mCherry expression in stress- and DAMGO-responsive monosynaptic VTA afferents. **(B)** Bar chart of area-divided quantification of stress- and DAMGO-TRAPed VTA inputs (stress: *n* = 6 per group, DAMGO: *n* = 6 per group). Data are presented as mean +SEM with individual data points (mice) shown alongside of the bars. Statistics: Two-Way ANOVA and Bonferroni *post-hoc* test. **(C)** Bar chart of absolute quantification of stress- and DAMGO-TRAPed VTA inputs (stress: *n* = 6 per group, DAMGO: *n* = 6 per group). Data are presented as mean +SEM with individual data points (mice) shown alongside of the bars, ** $P <$ 0.01. Statistics: Two-Way ANOVA and Bonferroni *post-hoc* test. **(D)** Bar chart of fractional quantification of stress- and DAMGO-TRAPed VTA inputs (stress: *n* = 6 per group, DAMGO: *n* = 6 per group). Data are presented as mean +SEM, ***$P <$ 0.001. Statistics: Two-Way ANOVA and Bonferroni *post-hoc* test. **(E)** Representative images of mPFC, RMTg, DR, vlPAG, PPTg and LTDg sections expressing mCherry from stress- and DAMGO-exposed TRAP2 animals. Abbreviations; IPN: interpeduncular nucleus, Aq: aqueduct; xscp: superior cerebellar peduncle. Scale bars: 500 (mPFC), 250 (RMTg), 250 (DR), 250 (vlPAG), PPTg (250 and 250 (LTDg) microns.

**Chemogenetic silencing of a $VTA_{SDS}$-ensemble Blocked Acute Social Defeat Stress-Conditioned Place Aversion**

Increased excitability of neurons projecting to the VTA is associated with the expression of SDS-driven behavioural aberrations (Fernandez et al., 2018; Linders et al., 2022). It has recently been demonstrated in TRAP2 mice that the $VTA_{SDS}$-ensemble exhibits increased neuronal excitability after acute SDS (Koutlas et al., 2022) . Therefore, we wondered whether inhibiting the $VTA_{SDS}$-ensemble during acute SDS affects the manifestation of stress-dependent behavioural phenotypes. To achieve this, we injected TRAP2 mice in the VTA with a rAAV2 carrying a Cre-dependent h4MDi-mCherry or mCherry (control group) transgene and exposed them to acute SDS 4 weeks later followed by a 4-OHT injection (Fig. 3A). hM4Di expression was validated in the VTA afterwards (Fig. 3C).

We first assessed whether inhibiting the $VTA_{SDS}$-ensemble would have an effect an effect on acute SDS-dependent place aversion, which we tested in a CPA paradigm [Fig. 4A, B(bottom)].
We observed that control animals spent significantly less time in the compartment in which they were previously experienced acute SDS, whereas hM4Di animals spent an equal amount of time in control and stress compartment [Main effect virus, $F_{(1,22)} = 0.43$, $P = 0.0002$; Fig 3D]. This indicates that inhibiting the $VTA_{SDS}$-ensemble completely abolishes acute SDS-induced place aversion, meaning that activity of these neurons is crucial for establishing an associative, short-term aversive memory.

Next we assessed whether $VTA_{SDS}$-ensemble silencing has an effect anxiety levels after acute SDS. To this end, we injected TRAP2 mice with c21 before exposing them to the acute SDS paradigm, whereafter we directly placed them in the open field arena to track their movement [Fig. 3A, B (middle)]. We did not observe a difference between hM4Di and mCherry animals in terms of time spent in the center region and locomotion, suggesting that inactivation of the $VTA_{SDS}$-ensemble does not alter the degree of anxiety following acute SDS (Fig. 3E)

It has been previously shown that other forms of acute stress result in reduced food intake in rats (Calvez et al., 2011), leading us to presume that acute SDS might cause the same effect. Therefore, we aimed to determine the effect of acute SDS on fat intake and the role of the $VTA_{SDS}$-ensemble in this behavioural phenotype. We addressed this issue by exposing the TRAP2 mice to a fat binge-like paradigm, in which fat intake after acute SDS was measured and compared to baseline fat intake established during prior non-stressed days [Fig. 3A, B(top)]. This experiment was performed in a counter-balanced manner, so that fat intake after acute SDS was measured twice per animal: one time after saline injection, and one time after c21 injection. We found that both mCherry [Main effect treatment, $F_{(1.999, 19.99)} = 28{,}91$ $P < 0.0001$; Fig. 4F] and hM4Di [Main effect treatment, $F_{(2, 36)} = 14.12$, $P < 0.0001$; Fig. 4G ) animals, regardless of whether they were injected with saline or c21, significantly decreased their fat intake after acute SDS in comparison to baseline. Therefore, these results imply that $VTA_{SDS}$-ensemble inhibition during acute SDS does not alleviate the consequential decline in fat intake.

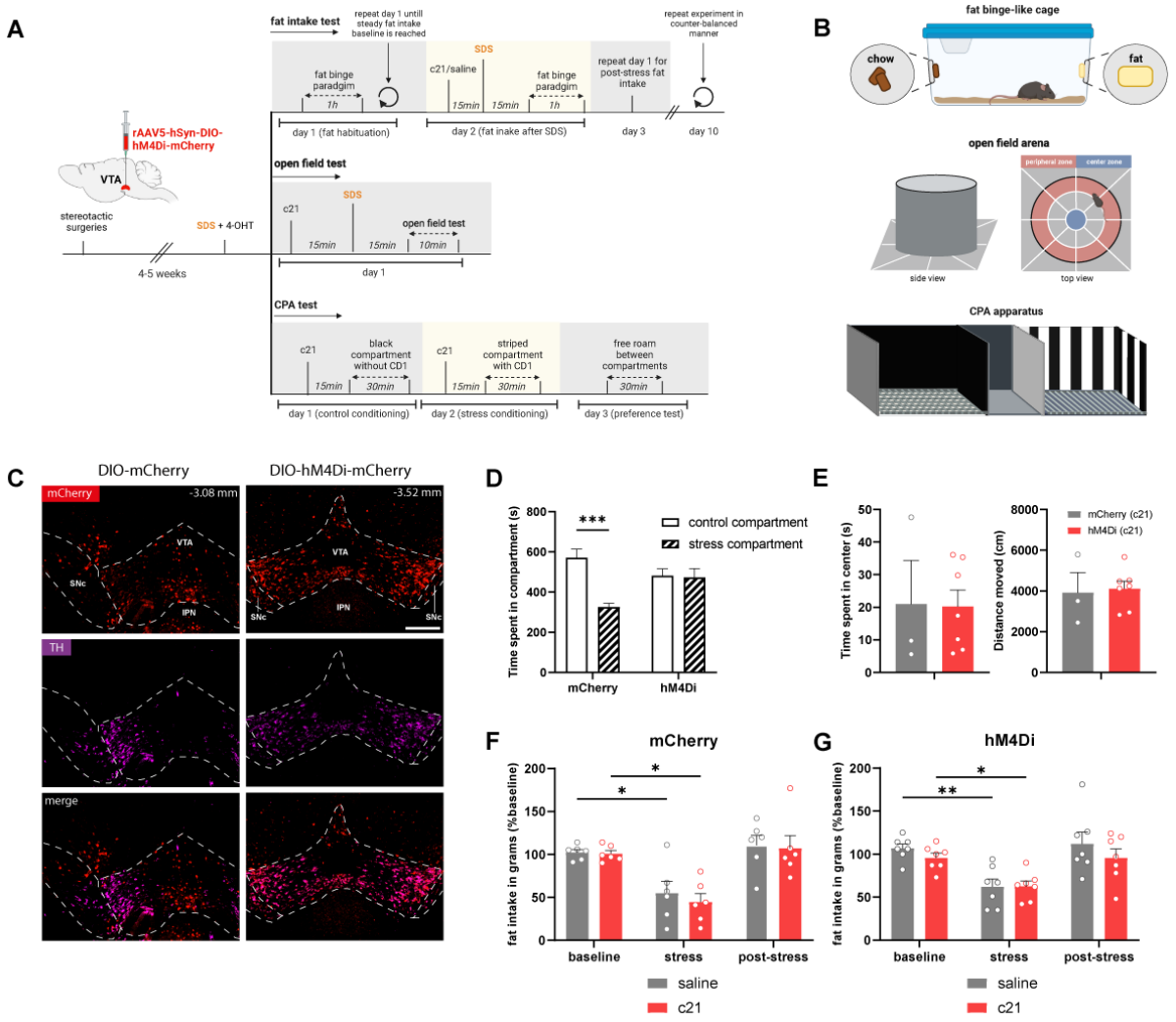


**Figure 3.** Behavioural effects of inhibiting the $VTA_{SDS}$-ensemble. **(A)** Experimental timelines of the fat binge-like paradigm, open field test and the conditioned place preference test. **(B)** Schematic illustrations of the fat binge-like cage (top), open field arena (middle) and conditioned place preference apparatus (bottom). **(C)** Representative images of (hM4Di-)mCherry expressing and dopaminergic neurons in the VTA of TRAP2 mice that underwent acute social defeat stress. Scale bar: 250 microns. **(D)** Bar chart of time spent in the neutral and stress compartment (mCherry: *n* = 6 per group, hM4Di: *n* = 7 per group). Data are presented as mean +SEM. ***$P$ < 0.001. Statistics: Two-Way ANOVA and Bonferroni *post-hoc* test. **(E)** Bar chart of time spent in the center zone of the open field arena (left) and total distance moved (right) during the open field test (mCherry: *n* = 3 per group, hM4Di: *n* = 7 per group). Data are presented as mean +SEM with individual data points (mice) shown alongside of the bars. Statistics: Two-Way ANOVA and Bonferroni *post-hoc* test. **(F)** Bar chart of fat intake relative to baseline in mCherry animals (saline: *n* = 6 per group, c21: *n* = 7 per group). Data are presented as mean +SEM with individual data points (mice) shown alongside of the bars, **$P$ < 0.01, ***$P$ < 0.001. Statistics: Two-Way ANOVA and Bonferroni *post-hoc* test. **(G)** Bar chart of fat intake relative to baseline in hM4Di animals (saline: *n* = 7 per group, c21: *n* = 7 per group). Data are presented as mean +SEM with individual data points (mice) shown alongside of the bars, *$P$ < 0.05, **$P$ < 0.01. Statistics: Two-Way ANOVA and Bonferroni *post-hoc* test.

**DISCUSSION**

In the present study, we used TRAP2xAi14 transgenic reporter mice to identify and compare acute SDS- and DAMGO-responsive neuronal ensembles in brain regions that project to the VTA. Furthermore, we injected a retrogradely-transported virus in the VTA of TRAP2 mice to enable detection and comparison of acute SDS- and DAMGO-activated monosynaptic VTA inputs, and found that in most cases, activation of VTA-projecting ensembles could not explain the previously observe difference. We also leveraged TRAP2 to gain chemogenetic control over an $VTA_{SDS}$-ensemble, and demonstrate that the functionality of this ensemble is crucial in associative learning. These findings will be further discussed below.

Our results demonstrate that acute SDS leads to increased neuronal activation in the mPFC, NAc, LH, BNST, VP and Hb in comparison to DAMGO or neutral stimuli. This is in line with another study that reported increased Fos immunoreactivity in the same regions after a similar acute SDS paradigm in rats, as compared to individually housed control animals (Lkhagvasuren et al., 2014). Furthermore, we found that DAMGO and neutral stimuli, resulted in similar neuronal activity levels in all quantified brain regions. This is surprising, since multiple studies have consistently reported increased neuronal activity in several brain regions after DAMGO administration, as measured by Fos expression (Campos-Jurado et al., 2019; DenBleyker et al., 2009; Zhang & Kelley, 2000). However, it should be noted that in these studies DAMGO was administered through brain-region specific infusion, whereas we injected DAMGO systemically. Moreover, it appears that DAMGO-induced neuronal activation differs based on the region of infusion. For instance, DAMGO infusion in the NAc strongly induced increased Fos expression in several brain regions, while targeting the dorsal striatum for infusion did not produce such effects (Zhang & Kelley, 2000).

In terms of brain region-specific neuronal populations that project directly to the VTA, we show that acute SDS only led to an increased activation in mPFC to VTA inputs when compared to DAMGO. Notably, out of all quantified inputs to the VTA, we detected the highest mCherry expression in the mPFC in all conditions, meaning that afferents from the mPFC constitute the highest fraction of acute SDS- and DAMGO-responsive VTA inputs. This is interesting, since other large-scale VTA inputs tracing studies indicate that the number of PFC to VTA projections, which are predominantly glutamatergic, is relatively low compared to other regions (Faget et al., 2016; Watabe-Uchida et al., 2012). These incongruities may be explained by the difference in retrograde vector, because the aforementioned studies both used a glycoprotein-deleted rabies virus. In fact, is has been previously demonstrated in the LH that rabies virus and rAAV-retro exhibit differences in neurotropism, causing discrepancies in mono-synaptic circuit labelling (Sun et al., 2019). For instance, input-labelling with rabies-virus yielded sparse expression in the mPFC, but high expression in the NAc. In a contrasting fashion, rAAV-dependent expression was high in the mPFC, but absent in the NAc. The latter observation, although concerning inputs to the LH, could be an explanation as to why we did not detect any mCherry expression in the NAc. Altogether, these incongruities stipulate the importance of utilizing different retrograde tracers and identifying differences in viral neurotropism in order to draw reliable conclusions from such data.

While our results displayed no difference in VTA input activity between acute SDS and DAMGO (except for the mPFC), it should be considered that the distinctions may reside within molecular subtypes of the VTA-projecting cells, which were not characterized in this study. For example, optogenetic excitation of GABAergic LH to VTA inputs produced CPP, whereas glutamatergic LH to VTA inputs elicited CPA (Nieh et al., 2016). In a similar fashion, photoactivation of GABAergic and glutamatergic BNST inputs to the VTA evoke CPP and CPA respectively (Jennings et al., 2013). Hypothetically speaking, one might therefore expect differential activation between glutamatergic and GABAergic subclasses of VTA-protecting neurons in the LH and BNST in response to acute SDS or DAMGO.

We wanted to understand the functional contribution of social stress-responsive neurons in the VTA during the development of acute SDS-driven behavioural phenotypes. To that end, we demonstrated that inactivation of the $VTA_{SDS}$-ensemble prevents acute SDS-induced CPA. This finding implies an important role of the $VTA_{SDS}$-ensemble in consolidation of an aversive associative memory. In support of this notion, it has been established that the VTA innervates the hippocampus through different subtypes of projections, and that these projections are considerably involved in learning and memory (Duszkiewicz et al., 2019; Ntamati & Lüscher, 2016; Tsetsenis et al., 2023). Moreover, a recent study in rats showed that bilateral infusion of DA receptor antagonist SCH 23390 in the dorsal hippocampus impaired place aversion in a mild CPA protocol (Kramar et al., 2021). Taking into account that the VTA is one of the main sources of DA release in in the hippocampus (Tsetsenis et al., 2023), this observation suggests that DAergic projection from to VTA to the hippocampus are essential in memory consolidation.

We also found that inhibiting the $VTA_{SDS}$-ensemble did not alleviate anxious behaviour and decreased fat intake after acute SDS, suggesting that these behavioural responses to stress are governed by neuronal circuits that do not necessarily require activity of the $VTA_{SDS}$-ensemble. However, it is important to bear in mind that we measured the effects of $VTA_{SDS}$-ensemble inhibition on fat consumption and anxiety 1 h (at maximum) after the acute SDS episode. At this time point, corticosterone plasma levels are peaking as a results of hyperactivity of the hypothalamic-pituitary-adrenal (HPA)-axis (Keeney et al., 2006). For this reason, it is presumable that the HPA-axis plays an important role in the development of anxiety and fat hypophagia after acute SDS. In fact, mRNA levels of corticotropin-releasing factor (CRF), which is another hormone produced by the HPA-axis, are also elevated after acute SDS, and CRF in turn acts on multiple regions in the brain to induce anxiety (Henckens et al., 2016; Keeney et al., 2006) This might explain why solely inhibiting the $VTA_{SDS}$-ensemble is not sufficient to alleviate stress-induced anxiety, as the role of VTA could be overshadowed by hyperactivity of the HPA-axis. In a similar fashion, CRF is known to induce anorexigenic responses through multiple targets in brain (Stengel & Taché, 2014). Whether CRF acts on the VTA to reduce food intake has not been explicitly described before, although there is some evidence from a study that links a potential role of the VTA to CRF-induced decrease in food reward (Wanat et al., 2013). Their work demonstrated that an acute CRF injection into the VTA reduced dopamine release in the NAc upon food reward delivery in rats on a mild food restriction. Taken together, the abovementioned results infer that the wide-spread effects of the stress-activated HPA axis might predominantly govern the short-term behavioural adaptations to acute SDS. Therefore, it would be interesting to also explore the role of the $VTA_{SDS}$-ensemble in stress-induced alterations in fat intake and anxiety at a later timepoint after the last stressful experience. In that regard, inhibiting the $VTA_{SDS}$-ensemble during a two-day repeated SDS paradigm, wherein the effects of stress on fat intake and anxiety are measured 24 after the last stress episode, would be a suitable follow-up experiment. Interestingly, the repeated stress paradigm leads to increased fat consumption in mice, rather than a decrease as we observed in the acute SDS paradigm (Linders et al., 2022). This stress-dependent increased fat consumption is driven by plasticity changes in the LH to VTA pathway, but the role of the $VTA_{SDS}$-ensemble in this behavioural effect remains yet to be addressed.

In sum, this study establishes a characterization of stress- and reward-responsive neuronal ensembles in brain regions that project to the VTA in terms of general activation and input-specific activation. The results indicate that acute SDS engages most regions substantially more than DAMGO, and that this effect was only reciprocated in VTA-projecting neuronal populations in the mPFC. The study also provides evidence for an essential role of the $VTA_{SDS}$-ensemble in the encoding a context-specific aversive association. These insights will pave the way for future studies addressing the interactions between stress- and reward-encoding neuronal circuits, ultimately contributing to the comprehension of psychopathological diseases, such as binge eating disorder, depression and drug addiction.

**REFERENCES**


Baik, J. H. (2020). Stress and the dopaminergic reward system. *Experimental & Molecular Medicine 2020 52:12*, *52*(12), 1879–1890. https://doi.org/10.1038/s12276-020-00532-4

Calvez, J., Fromentin, G., Nadkarni, N., Darcel, N., Even, P., Tomé, D., … Chaumontet, C. (2011). Inhibition of food intake induced by acute stress in rats is due to satiation effects. *Physiology & Behavior*, *104*(5), 675–683. https://doi.org/10.1016/J.PHYSBEH.2011.07.012

Campos-Jurado, Y., Igual-López, M., Padilla, F., Zornoza, T., Granero, L., Polache, A., … Hipólito, L. (2019). Activation of MORs in the VTA induces changes on cFos expression in different projecting regions: Effect of inflammatory pain. *Neurochemistry International*, *131*, 104521. https://doi.org/10.1016/J.NEUINT.2019.104521

Chaudhury, D., Walsh, J. J., Friedman, A. K., Juarez, B., Ku, S. M., Koo, J. W., … Han, M. H. (2012). Rapid regulation of depression-related behaviours by control of midbrain dopamine neurons. *Nature 2012 493:7433*, *493*(7433), 532–536. https://doi.org/10.1038/nature11713

Del Arco, A., Park, J., & Moghaddam, B. (2020). Unanticipated Stressful and Rewarding Experiences Engage the Same Prefrontal Cortex and Ventral Tegmental Area Neuronal Populations. *ENeuro*, *7*(3), 1–13. https://doi.org/10.1523/ENEURO.0029-20.2020

DeNardo, L. A., Liu, C. D., Allen, W. E., Adams, E. L., Friedmann, D., Fu, L., … Luo, L. (2019). Temporal evolution of cortical ensembles promoting remote memory retrieval. *Nature Neuroscience 2019 22:3*, *22*(3), 460–469. https://doi.org/10.1038/s41593-018-0318-7

DenBleyker, M., Nicklous, D. M., Wagner, P. J., Ward, H. G., & Simansky, K. J. (2009). Activating μ-opioid receptors in the lateral parabrachial nucleus increases c-Fos expression in forebrain areas associated with caloric regulation, reward and cognition. *Neuroscience*, *162*(2), 224–233. https://doi.org/10.1016/J.NEUROSCIENCE.2009.04.071

Duszkiewicz, A. J., McNamara, C. G., Takeuchi, T., & Genzel, L. (2019). Novelty and Dopaminergic Modulation of Memory Persistence: A Tale of Two Systems. *Trends in Neurosciences*, *42*(2), 102–114. https://doi.org/10.1016/J.TINS.2018.10.002

Faget, L., Osakada, F., Duan, J., Ressler, R., Johnson, A. B., Proudfoot, J. A., … Hnasko, T. S. (2016). Afferent Inputs to Neurotransmitter-Defined Cell Types in the Ventral Tegmental Area. *Cell Reports*, *15*(12), 2796–2808. https://doi.org/10.1016/J.CELREP.2016.05.057

Fernandez, S. P., Broussot, L., Marti, F., Contesse, T., Mouska, X., Soiza-Reilly, M., … Barik, J. (2018). Mesopontine cholinergic inputs to midbrain dopamine neurons drive stress-induced depressive-like behaviors. *Nature Communications 2018 9:1*, *9*(1), 1–12. https://doi.org/10.1038/s41467-018-06809-7

Fields, H. L., & Margolis, E. B. (2015). Understanding opioid reward. *Trends in Neurosciences*, *38*(4), 217–225. https://doi.org/10.1016/J.TINS.2015.01.002

Goto, T., Kubota, Y., Tanaka, Y., Iio, W., Moriya, N., & Toyoda, A. (2014). Subchronic and mild social defeat stress accelerates food intake and body weight gain with polydipsia-like features in mice. *Behavioural Brain Research*, *270*, 339–348. https://doi.org/10.1016/J.BBR.2014.05.040

Henckens, M. J. A. G., Deussing, J. M., & Chen, A. (2016). Region-specific roles of the corticotropin-releasing factor–urocortin system in stress. *Nature Reviews Neuroscience 2016 17:10*, *17*(10), 636–651. https://doi.org/10.1038/nrn.2016.94

Holly, E. N., & Miczek, K. A. (2016). Ventral tegmental area dopamine revisited: effects of acute and repeated stress. *Psychopharmacology*, *233*(2), 163–186. https://doi.org/10.1007/S00213-015-4151-3

Jennings, J. H., Sparta, D. R., Stamatakis, A. M., Ung, R. L., Pleil, K. E., Kash, T. L., & Stuber, G. D. (2013). Distinct extended amygdala circuits for divergent motivational states. *Nature 2013 496:7444*, *496*(7444), 224–228. https://doi.org/10.1038/nature12041

Johnston, C. E., Herschel, D. J., Lasek, A. W., Hammer, R. P., & Nikulina, E. M. (2015). Knockdown of ventral tegmental area mu-opioid receptors in rats prevents effects of social defeat stress: implications for amphetamine cross-sensitization, social avoidance, weight regulation and expression of brain-derived neurotrophic factor. *Neuropharmacology*, *89*, 325–334. https://doi.org/10.1016/J.NEUROPHARM.2014.10.010

Keeney, A., Jessop, D. S., Harbuz, M. S., Marsden, C. A., Hogg, S., & Blackburn-Munro, R. E. (2006). Differential Effects of Acute and Chronic Social Defeat Stress on Hypothalamic-Pituitary-Adrenal Axis Function and Hippocampal Serotonin Release in Mice. *Journal of Neuroendocrinology*, *18*(5), 330–338. https://doi.org/10.1111/J.1365-2826.2006.01422.X

Koutlas, I., Linders, L. E., van der Starre, S. E., Wolterink-Donselaar, I. G., Adan, R. A. H., & Meye, F. J. (2022).

Characterizing and TRAPing a Social Stress-Activated Neuronal Ensemble in the Ventral Tegmental Area. *Frontiers in Behavioral Neuroscience*, *16*. https://doi.org/10.3389/FNBEH.2022.936087/FULL

Kramar, C. P., Castillo-Díaz, F., Gigante, E. D., Medina, J. H., & Barbano, M. F. (2021). The late consolidation of an aversive memory is promoted by VTA dopamine release in the dorsal hippocampus. *European Journal of Neuroscience*, *53*(3), 841–851. https://doi.org/10.1111/EJN.15076

Lammel, S., Lim, B. K., Ran, C., Huang, K. W., Betley, M. J., Tye, K. M., … Malenka, R. C. (2012). Input-specific control of reward and aversion in the ventral tegmental area. *Nature 2012 491:7423*, *491*(7423), 212–217. https://doi.org/10.1038/nature11527

Lamonte, N., Echo, J. A., Ackerman, T. F., Christian, G., & Bodnar, R. J. (2002). Analysis of opioid receptor subtype antagonist effects upon mu opioid agonist-induced feeding elicited from the ventral tegmental area of rats. *Brain Research*, *929*(1), 96–100. https://doi.org/10.1016/S0006-8993(01)03382-0

Linders, L. E., Patrikiou, L., Soiza-Reilly, M., Schut, E. H. S., van Schaffelaar, B. F., Böger, L., … Meye, F. J. (2022). Stress-driven potentiation of lateral hypothalamic synapses onto ventral tegmental area dopamine neurons causes increased consumption of palatable food. *Nature Communications 2022 13:1*, *13*(1), 1–19. https://doi.org/10.1038/s41467-022-34625-7

Lkhagvasuren, B., Oka, T., Nakamura, Y., Hayashi, H., Sudo, N., & Nakamura, K. (2014). Distribution of Fos-immunoreactive cells in rat forebrain and midbrain following social defeat stress and diazepam treatment. *Neuroscience*, *272*, 34–57. https://doi.org/10.1016/J.NEUROSCIENCE.2014.04.047

Meye, F. J., & Adan, R. A. H. (2014). Feelings about food: the ventral tegmental area in food reward and emotional eating. *Trends in Pharmacological Sciences*, *35*(1), 31–40. https://doi.org/10.1016/J.TIPS.2013.11.003

Morales, M., & Margolis, E. B. (2017). Ventral tegmental area: cellular heterogeneity, connectivity and behaviour. *Nature Reviews Neuroscience 2017 18:2*, *18*(2), 73–85. https://doi.org/10.1038/nrn.2016.165

Nieh, E. H., Vander Weele, C. M., Matthews, G. A., Presbrey, K. N., Wichmann, R., Leppla, C. A., … Tye, K. M. (2016). Inhibitory Input from the Lateral Hypothalamus to the Ventral Tegmental Area Disinhibits Dopamine Neurons and Promotes Behavioral Activation. *Neuron*, *90*(6), 1286–1298. https://doi.org/10.1016/J.NEURON.2016.04.035

Nikulina, E. M., Hammer, R. P., Miczek, K. A., & Kream, R. M. (1999). Social defeat stress increases expression of mu-opioid receptor mRNA in rat ventral tegmental area. *Neuroreport*, *10*(14), 3015–3019. https://doi.org/10.1097/00001756-199909290-00026

Ntamati, N. R., & Lüscher, C. (2016). VTA Projection Neurons Releasing GABA and Glutamate in the Dentate Gyrus. *ENeuro*, *3*(4). https://doi.org/10.1523/ENEURO.0137-16.2016

Patki, G., Solanki, N., Atrooz, F., Allam, F., & Salim, S. (2013). Depression, anxiety-like behavior and memory impairment are associated with increased oxidative stress and inflammation in a rat model of social stress. *Brain Research*, *1539*, 73–86. https://doi.org/10.1016/J.BRAINRES.2013.09.033

Root, D. H., Barker, D. J., Estrin, D. J., Miranda-Barrientos, J. A., Liu, B., Zhang, S., … Morales, M. (2020). Distinct Signaling by Ventral Tegmental Area Glutamate, GABA, and Combinatorial Glutamate-GABA Neurons in Motivated Behavior. *Cell Reports*, *32*(9), 108094. https://doi.org/10.1016/J.CELREP.2020.108094

Schindelin, J., Arganda-Carreras, I., Frise, E., Kaynig, V., Longair, M., Pietzsch, T., … Cardona, A. (2012). Fiji - an Open Source platform for biological image analysis. *Nature Methods*, *9*(7), 676–682. https://doi.org/10.1038/NMETH.2019

Sinha, R., & Jastreboff, A. M. (2013). Stress as a Common Risk Factor for Obesity and Addiction. *Biological Psychiatry*, *73*(9), 827–835. https://doi.org/10.1016/J.BIOPSYCH.2013.01.032

Smith, A., Hyland, L., Al-Ansari, H., Watts, B., Silver, Z., Wang, L., … Abizaid, A. (2023). Metabolic, neuroendocrine and behavioral effects of social defeat in male and female mice using the chronic non-discriminatory social defeat stress model. *Hormones and Behavior*, *155*. https://doi.org/10.1016/J.YHBEH.2023.105412

Stengel, A., & Taché, Y. (2014). CRF and urocortin peptides as modulators of energy balance and feeding behavior during stress. *Frontiers in Neuroscience*, *8*(8 MAR), 78583. https://doi.org/10.3389/FNINS.2014.00052/BIBTEX

Sun, L., Tang, Y., Yan, K., Yu, J., Zou, Y., Xu, W., … Cao, G. (2019). Differences in neurotropism and neurotoxicity among retrograde viral tracers. *Molecular Neurodegeneration*, *14*(1). https://doi.org/10.1186/S13024-019-0308-6

Tsetsenis, T., Broussard, J. I., & Dani, J. A. (2023). Dopaminergic regulation of hippocampal plasticity, learning, and memory. *Frontiers in Behavioral Neuroscience*, *16*, 1092420. https://doi.org/10.3389/FNBEH.2022.1092420/BIBTEX

Wanat, M. J., Bonci, A., & Phillips, P. E. M. (2013). CRF acts in the midbrain to attenuate accumbens dopamine

release to rewards but not their predictors. *Nature Neuroscience*, *16*(4). https://doi.org/10.1038/nn.3335
Watabe-Uchida, M., Zhu, L., Ogawa, S. K., Vamanrao, A., & Uchida, N. (2012). Whole-Brain Mapping of Direct Inputs to Midbrain Dopamine Neurons. *Neuron*, *74*(5), 858–873. https://doi.org/10.1016/J.NEURON.2012.03.017
Zhang, M., & Kelley, A. E. (2000). Enhanced intake of high-fat food following striatal mu-opioid stimulation: microinjection mapping and Fos expression. *Neuroscience*, *99*(2), 267–277. https://doi.org/10.1016/S0306-4522(00)00198-6
Zhang, Y., Landthaler, M., Schlussman, S. D., Yuferov, V., Ho, A., Tuschl, T., & Kreek, M. J. (2009). Mu opioid receptor knockdown in the substantia nigra/ventral tegmental area by synthetic small interfering RNA blocks the rewarding and locomotor effects of heroin. *Neuroscience*, *158*(2), 474–483. https://doi.org/10.1016/J.NEUROSCIENCE.2008.09.039

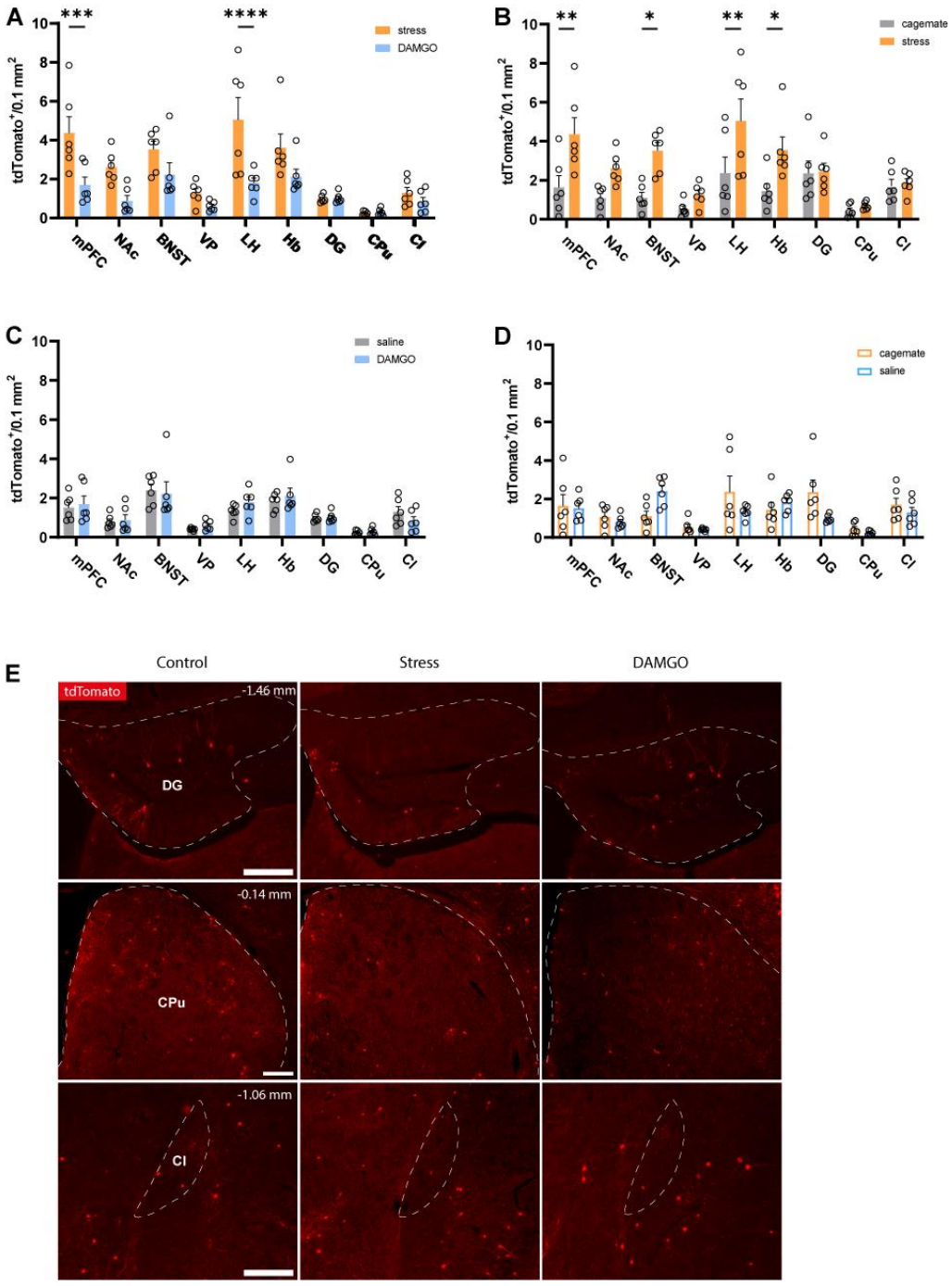


**Supplementary Figure 1. (A)** Bar chart quantification of stress- and DAMGO-TRAPed neurons in a several brain regions (stress: *n* = 6 per group, DAMGO: *n* = 6 per group). Data are presented as mean +SEM with individual data points (mice) shown alongside of the bars, ***$P < 0.001$, **** $P < 0.0001$. Statistics: Two-Way ANOVA and Bonferroni *post-hoc* test. **(B)** Bar chart quantification of cage mate- and stress-TRAPed neurons in a several brain regions (cage mate: *n* = 6 per group, stress: *n* = 6 per group). Data are presented as mean +SEM with individual data points (mice) shown alongside of the bars , *$P < 0.05$, ** $P < 0.01$. Statistics: Two-Way ANOVA and Bonferroni *post-hoc* test. **(C)** Bar chart quantification of saline- and DAMGO-TRAPed neurons in a several brain regions (saline: *n* = 6 per group, DAMGO: *n* = 6 per group). Data are presented as mean +SEM with individual data points (mice) shown alongside of the bars. Statistics: Two-Way ANOVA and Bonferroni *post-hoc* test**. (D)** Bar chart quantification of cage mate- and saline-TRAPed neurons in a several brain regions (cage mate: *n* = 6 per group, saline: *n* = 6 per group). Data are presented as mean +SEM with individual data points (mice) shown alongside of the bars. Statistics: Two-Way ANOVA and Bonferroni *post-hoc* test. **(E)** Representative images of DG, CPu and Cl sections expressing tdTomato from neutral-, stress- and DAMGO-exposed TRAP2xAi14 animals. Scale bar: 250 microns.

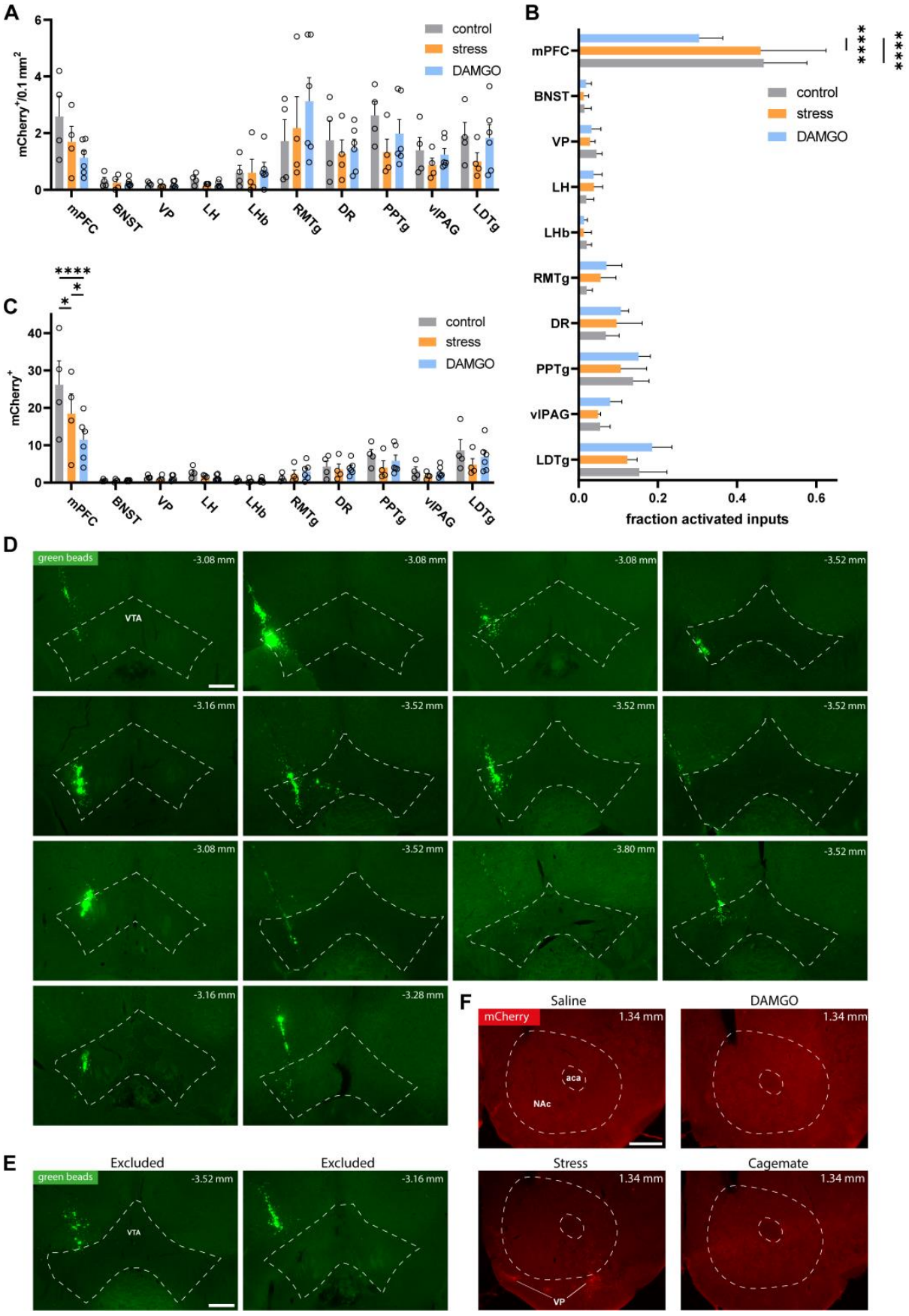
A
mCherry+/0.1 mm2
control
stress
DAMGO
mPFC
BNST
VP
LH
LHb
RMTg
DR
PPTg
vlPAG
LDTg
B
fraction activated inputs
C
mCherry+
D
green beads
VTA
E
Excluded
F
Saline
DAMGO
Stress
Cagemate
mCherry
aca
NAc
VP
1.34 mm

**Supplementary Figure 2. (A)** Bar chart of area-divided quantification of neutral-, stress- and DAMGO-TRAPed VTA inputs (neutral: n =4 per group, stress: *n* = 6 per group, DAMGO: *n* = 6 per group). Data are presented as mean +SEM with individual data points (mice) shown alongside of the bars. Statistics: Two-Way ANOVA and Bonferroni *post-hoc* test. **(B)** Bar chart of absolute quantification of neutral-, stress- and DAMGO-TRAPed VTA inputs (neutral: n =4 per group, stress: *n* = 6 per group, DAMGO: *n* = 6 per group). Data are presented as mean +SEM, **P* < 0.05, ** *P* < 0.01, ****P* < 0.001. Statistics: Two-Way ANOVA and Bonferroni *post-hoc* test**. (C)** Bar chart of fractional quantification of neutral-, stress- and DAMGO-TRAPed VTA inputs (neutral: n =4 per group, stress: *n* = 6 per group, DAMGO: *n* = 6 per group). Data are presented as mean +SEM, ****P* < 0.001, *****P* < 0.0001 . Statistics: Two-Way ANOVA and Bonferroni *post-hoc* test **(D)** Representative images of sections with fluorescent green beads in the VTA of included animals. Scalebar: 250 microns. **(F)** Representative images of NAc sections expressing no mCherry from TRAP2 animals from all conditions. Scalebar: 500 microns. **(E)** Representative images of VTA sections with fluorescent green beads of excluded animals. Scalebar: 250 microns.